Autonomous Multilateral Surgical Tumor Resection with Interchangeable Instrument Mounts and Fluid Injection Device

Stephen McKinley[1], Animesh Garg[2], Siddarth Sen[3], David V. Gealy[1],
Jonathan P. McKinley[1], Yiming Jen[3], Ken Goldberg[2]

***Abstract*— Supervised automation of selected subtasks in Robot-Assisted Minimally Invasive Surgery (RMIS) has potential to reduce surgeon fatigue, operating time, and facilitate tele-surgery. Tumor resection is a multi-step multilateral surgical procedure to localize, expose, and debride (remove) a subcutaneous tumor, then seal the resulting wound with surgical adhesive. We developed a finite state machine using the novel devices to autonomously perform the tumor resection. The first device is an interchangeable instrument mount which uses the jaws and wrist of a standard RMIS gripping tool to securely hold and manipulate a variety of end-effectors. The second device is a fluid injection system that can facilitate precision delivery of material such as chemotherapy, stem cells, and surgical adhesives to specific targets using a single-use needle attached using the interchangeable instrument mount. Fluid flow through the needle is controlled via an externally-mounted automated lead screw. Initial experiments suggest that an automated Intuitive Surgical dVRK system which uses these devices combined with a palpation probe and sensing model described in a previous paper can successfully complete the entire procedure in five of ten trials. We also show the most common failure phase, debridement, can be improved with visual feedback. Design details and video are available at: http://berkeleyautomation.github.io/surgical-tools.**

I. Introduction

Robotic Surgical Assistants (RSAs) are frequently used with high success rates for Robotic Minimally Invasive Surgical (RMIS) procedures such as prostectomy, uterectomy, and tumorectomy within the abdominal and thoracic cavities [8, 32]. Intuitive Surgical's *da Vinci* Robotic Surgical Assistant (RSA) facilitated over 570,000 procedures in 2014 with 3000 RSA systems worldwide [16]. RSAs are currently controlled by surgeons via pure tele-operation, requiring constant surgeon attention and control. Supervised autonomy of surgical sub-tasks has the potential to reduce surgeon tedium and fatigue, operating time, and to open the door to tele-surgery.

We consider the multilateral surgical procedure of Tumor Resection which includes four sub-tasks: (a) *Palpation*, (b) *Incision*, (c) *Debridement*, and (d) *Adhesive Injection*. These sub-tasks require several of the *Fundamental Skills of Robotic Surgery* (FSRS) [37] used for training laparoscopic surgeons [9, 36]. We explore the automation of this procedure using the da Vinci Surgical Research Kit (dVRK), a commercial RMIS system from Intuitive Surgical [1, 19].

The authors are with University of California, Berkeley, CA, USA
[1]Mechanical Engineering
{mckinley, dgealy, jmck11}@berkeley.edu
[2]IEOR & EECS, {animesh.garg, goldberg}@berkeley.edu
[3]EECS, {siddarthsen, yjen}@berkeley.edu

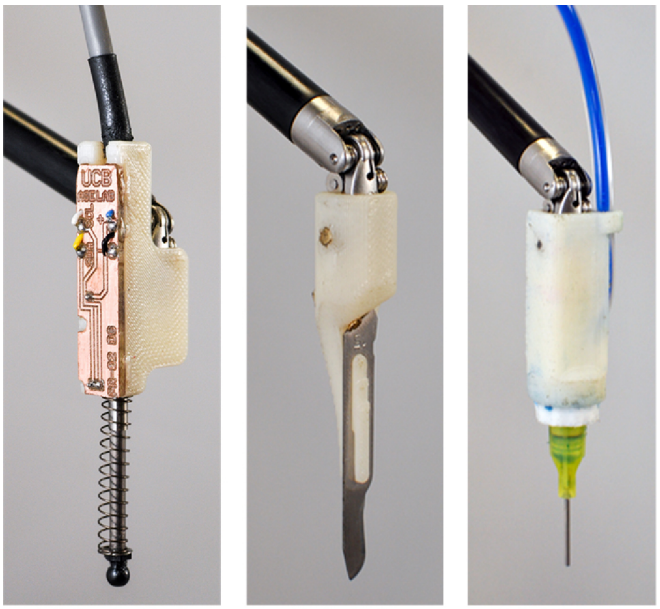

Fig. 1: a, b, c) da Vinci surgical retractor with three end-effector extensions; d) Surgical tumor resection overview.

Many surgical procedures require multiple instruments and changing instruments is time consuming. In 2009, Miller et al. [28] labeled video data to measure elapsed time of fourteen different laparoscopic surgical procedures; 24% of the total procedure time involved the task of changing instruments for specialized surgical sub-tasks. Miller et al. concluded surgery time and costs could be decreased by use of a quick-change instrument system: they proposed a concept for devices without wristed articulation. We have developed several novel devices, including an interchange-

Preprint submitted to 2016 IEEE International Conference on Robotics and Automation. Received September 15, 2015.

able low-cost instrument mount for retractors with wristed articulation as illustrated in Figures 1 and 3, to be used to explore automated tumor resection.

Contributions

1. Designs of two new interchangeable end-effector mechanical mounts.
2. Design of a precision fluid injector system.
3. Experiments with the above devices and finite state machine model on autonomous performance of surgical tumor resection experiments using silicone phantoms to evaluate feasibility and repeatability.

II. Related Work

A. Autonomous Multilateral Surgical Tumor Resection

Several researchers have explored autonomous performance of RMIS sub-tasks [3, 7, 41, 45]. Moustris et al. [29] and Kranzfelder et al. [23] provide reviews of recent developments in semi-autonomous and autonomous execution of various experimental and clinical surgical procedures. Academic availability of RSAs such as Intuitive Surgical's dVRK [19] and the Raven II [14] system have accelerated recent developments in surgical automation. This paper focuses on the task of *tumor resection* which includes four sub-tasks [10]: *Palpation*, *Incision*, *Debridement*, and *Injection*, using the finite element approach described in a previous work [30]. Our video, which demonstrated autonomous performance of this procedure in addition to several failure modes, won Best Video Award at the Hamlyn Surgical Robotics Workshop in June 2015 [27]. We also presented a paper on the palpation probe design and experiments in 2015 [26]. The present paper describes mechanical design of the interchangeable mount, a fluid injection device used for tumor resection, and data on experiments.

Tissue Palpation: Konstantinova et al. [22] provide an extensive survey on recent advances for sensor design and deployment to enable successful haptic palpation which is necessary for surgeons to find inclusions within tissues. Algorithms for active exploration in tumor localization [31] and tumor ablation [15] offer new methods to consider for improved robotic palpation outcomes. Sterilization of instruments remains a challenging limitation for clinical use of tactile force sensing in RMIS [5].

Autonomous Incision and Cutting: A variety of incising methods have been explored with the da Vinci including electrocautery and ultrasonic knives from Intuitive Surgical [2] as well as a da Vinci-mounted CO_2 laser used to incise tissue surrounding a tumor [24]. However, the use of lasers, electrocautery, or ultrasonic knives can produce more tissue damage and slower wound healing compared to scalpel incisions [13]. Scalpel instruments are available as standalone tools for the da Vinci. However, they do not allow for interchangeability of instrument-tips. We created a scalpel instrument-tip (shown in Figure 1(b)) compatible with the proposed instrument mount for use in the automated tumor resection pipeline as described in Section V.

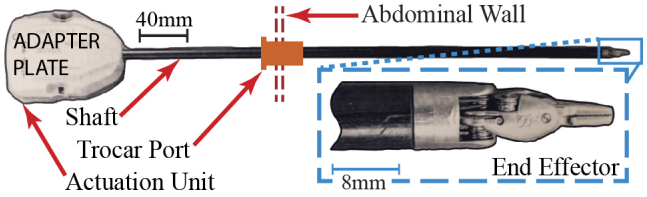

Fig. 2: A schematic view of a da Vinci Classic instrument inserted through a trocar port into the abdominal cavity.

Tissue Debridement: Surgical debridement is a tedious surgical sub-task in which foreign inclusions or damaged tissues are removed from the body [6, 12]. Automated brain tumor ablation and resection with the RAVEN II has been explored in simulation [15]. Kehoe et al. [20] used motion planning to perform multilateral surgical debridement using the Raven II surgical robot. We have explored tissue debridement and multilateral cutting on deformable materials with the dVRK [30].

Targeted Fluid Injection: Local delivery of fluids via direct injections allows for a controlled and precise delivery of materials such as chemotherapy drugs, surgical glues, and stem cells. However, delivery to organs in inaccessible locations such as in the thorax, abdomen and pelvis is challenging because of the relatively high degree of trauma required [18]. Non-MIS robot injection tools have been developed and evaluated in the past [39]. Robotic catheter injection tools have also been studied [4]. However, there is a need for low-cost RMIS compatible delivery devices which enable access to internal organs and deliver controlled quantities of localized fluids [17].

Wound Closure: There are a number of clinically used methods for wound closure including suturing, staples [44] and surgical adhesives. Padoy et al. [33] demonstrated execution of a human-robot collaborative suturing task on the dVRK platform. Surgical glue has been used successfully to close inter-cavity hernias [25], but little work exists on use of RSAs for precision application.

B. Interchangeable MIS Instrument Systems

There have been a number of studies on non-robotic laparoscopic instruments with interchangeable end-effectors [21, 34, 35]. However, the end-effectors of these instruments allow only a single degree-of-freedom (jaw opening/closing) and do not interface with existing surgical retractors. Most existing robotic systems such as the da Vinci and DLR MICA exchange the entire instrument instead of the end effector [2, 43].

Implementation of Interchangeable Systems: Currently, the instrument change procedure for the da Vinci RSA involves the complete removal of the instrument from within the abdominal cavity through the trocar port (see Figure 2). To make interchangeable instrument end-effectors beneficial to RMIS, end-effectors can be introduced through a separate utility trocar port as described in [38]. The utility trocar port can also be the point of entry for electronic cables and catheters as described in [21] allowing for sensorized and

Preprint submitted to 2016 IEEE International Conference on Robotics and Automation. Received September 15, 2015.

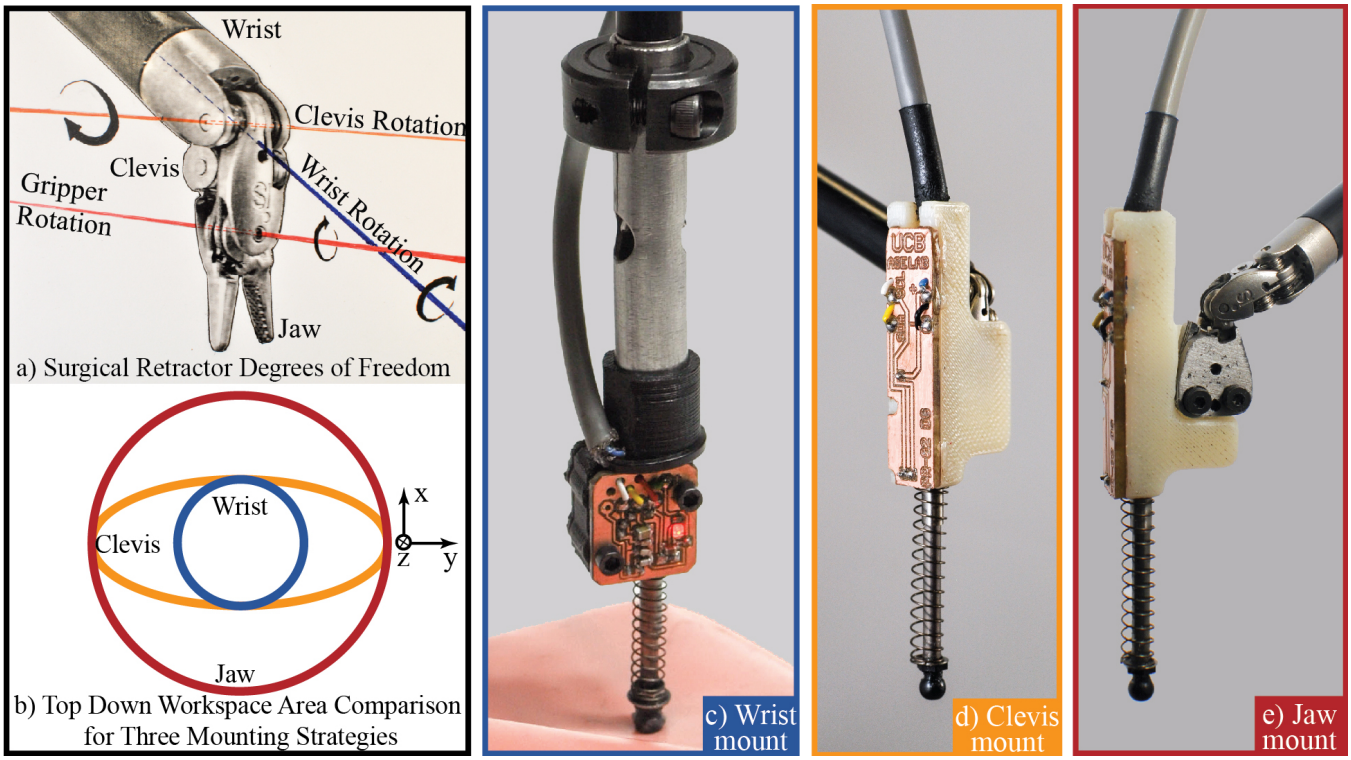

Fig. 3: Three designs for end-effector instrument mounts differentiated by attachment strategies to the surgical retractor. The usable workspace of the Palpation Probe decreases as degrees of freedom (a) are restricted. The surgical retractor in (c) extends axially within the mount. The retractor in (d) is inserted at level with the clevis pully seen in (a).

fluid delivery end-effectors to be introduced into the RMIS workspace.

Robotic Interchangeable Instrument Systems: In 2007, Friedman et al. proposed the early use of a robotic system to automate instrument change on the da Vinci RSA [11]. However, their method required additional automated infrastructure including an industrial arm used to change the entire da Vinci instrument after removing it from the abdominal cavity. Figure 2 shows a da Vinci classic needle driver.

Commercially Available Devices: In 2015, Teleflex Medical was granted FDA clearance to market interchangeable instrument-tips for *non-robotic* MIS instruments with a single degree of freedom [42]. Ethicon Medical [34] recently announced forthcoming percutaneous endoscopic instruments with interchangeable end-effectors which can be introduced via a trocar utility port. Percutaneous surgery (a subset of MIS) involves passing instrument shafts directly through the abdominal wall rather than inserting through an intermediate trocar port; as far as can be determined from the announcement, these end-effectors have a single controllable degree-of-freedom.

Existing non-robotic interchangeable instrument end-effectors do not build upon existing retractor geometry, limiting the combination of possible instrument configurations. Additionally, all of these devices allow only a single controllable degree-of-freedom at the instrument tip with similar limitations as in our initial design for a wrist mount (described in Figure 3(b) and shown in Figure 3(c)).

TABLE I: Comparison of Wrist, Clevis, and Jaw Mounting.

	Wrist Mount	Clevis Mount	Jaw Mount
Wrist Rotation	(full) 360°	(full) 360°	(full) 360°
Clevis Rotation	(none) 0°	(full) 180°	(full) 180°
Jaw Rotation	(none) 0°	(none) 0°	(restricted) 60°

III. System Design and Interfacing

The interchangeable mounts are designed to have the following characteristics:

1. Kinematically constrained mounting on a standard surgical retractor end-effector using existing geometric features
2. Self-actuating retractor fixation requiring minimal grip force
3. Preservation of existing retractor articulation
4. Form factor to fit through a 15 mm cannula during minimally invasive procedures
5. Low-cost for single-use disposability (to facilitate sterilization).

Using these criterion, we designed and evaluated three modes of mounting end effectors: (a) non-interchangeable mount, (b) an interchangeable clevis mount and (c) an interchangeable jaw mount.

A. Wrist Mount Design

We introduced a low-cost wrist-mounting design in our recent work for use as a minimally invasive palpation sensor [26] shown in Figure 3(c). However, due to the sleeve enclosure, the motion of the end-effector was restricted to only wrist rotation. This limited the range of motion of the

surgical retractor and area of total instrument workspace as illustrated in Figure 3(b).

B. Clevis Mount Design

We designed an interchangeable instrument-tip mount to address these limitations by mounting on the 'clevis' link of the surgical retractors (see Figure 3(a)) providing stabilization (as shown in Figure 3(d)). The cavity on the clevis mount (illustrated in Figure 4) was designed to help funnel the dVRK needle driver into its proper orientation, allowing a higher tolerance for misalignment in settings without visual feedback and easing the demands on software. The furthest proximal extent of the mount extends up to the clevis joint linkage; any further extension along this axis would limit clevis rotation as shown in Figure 3(b). The cavity of the mount mates with the side contour of the surgical retractor to limit rotation away from the 'z' axis (defined in Figure 4) yet maintains a sliding fit to allow the retractor to detach easily.

The internal cavity of the clevis mount is designed with locking pins extending from the walls of the interchangeable mount. The pins securely engage shoulders located on the retractor jaw when open (point A marked on Figure 4). The angle of these pins (angle 'γ' shown in Figure 4) matches the angle of the shoulders on the opened jaws to maximize contact area. A self-actuating lock is achieved as the points of contact on the jaw, which serves as a fulcrum, forces the jaws further open in contact with the internal cavity of the mount as a force in the positive 'z' direction is applied (shown in Figure 4). Movement in the negative 'z' direction is limited by contact between the clevis linkage and the internal cavity of the interchangeable mount.

The minimum angle of opening (and thus, the minimum cross-sectional area of the interchangeable clevis mount) is limited by the minimum jaw angle that disengages the locking pins. The maximal diameter of the mount is constrained by the surgical cannula diameter. The mount was prototyped with ABS plastic using a Stratysys uPrint 3D printer and two $00-80$ machine screws.

The clevis mount allows greater range of motion along the 'x-y' plane as shown in Figure 3(b); however, because jaw rotational motion was restricted, inaccuracies occurred along the 'x-z' plane. This limited the RSA's ability to work with clevis-mounted instrument extensions in the 'y' axis, and resulted in a workspace limited to a narrow ellipse along the 'x' axis as shown in Figure 3(b). Despite these limitations, we were able to demonstrate the utility of a self-engaging interchangeable instrument-tip mount by performing tumor resection surgeries in silicon flesh phantoms as described in Sections VI and V.

C. Jaw Mount Design

The jaw mount design was created to extend the utility of the clevis mount design by allowing greater range of motion in jaw rotation axes. Mount movement in the negative 'z' direction is constrained by an internal spur that mates with the 'palm' of the surgical retractor clevis between

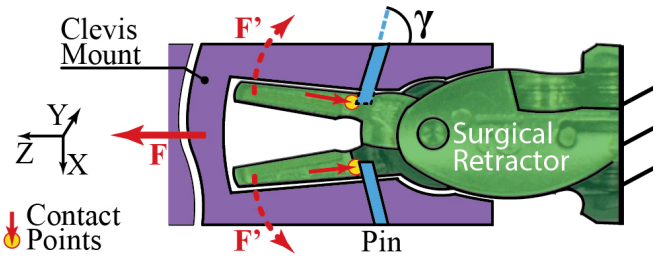

Fig. 4: A self-actuating mount: Force disturbance F in the negative z direction is countered by the contact points between the mount pins and the retractor shoulder. This results in an outwards clamping force F' to the clevis mount. The interchangeable mount can be designed with any external shape.

the two retractor jaws. The mating cavity was created by laminating water-jetted 1095 spring steel sheets of 0.025 *in* thickness using two M2 machine screws. Points to engage the retractor shoulders were designed integrally the laminate layers. Spring steel was chosen for initial prototypes because of its resilience at pin-points, and its high strength-to-volume ratio which allows for a decrease in overall size. However, this design may also be 3D-printed without any further fabrication considerations. This interchangeable mount is affixed to modular instrument tips and end-effectors as shown in Figure 3(e); custom instrument-tips can be integrated within the 3D-printed version of this mount.

IV. Fluid Injection Instrument

We designed an automated injection instrument with three components: end-effector mounted needle (seen in Figure 1(c)), a flexible catheter assembly, and a drive motor assembly (as seen in Figure 5) mounted to the upper portion of the dVRK arm behind the sterile barrier.

Typical local injection volume during stem cell therapy is on the order of 10's of milliliters, with per-injection doses of 10mL to 30mL representing approximately 10 million viable cells [40]; this volume dictated the maximum-volume design constraint of the injector and led to the use of a remote dVRK-mounted syringe pump rather than have the end-effector carry the payload.

The Fluid Injector precision constraint is guided by the dose volume of surgical glue (6 uL dose for each 2 mL of wound closure) [25]. Injection force is provided by a Haydon-Kerk 21F4AC-2.5 linear actuator, powered by Allegro's A4988 micro-stepping bipolar stepper motor driver, and controlled by an Arduino Pro Mini 328 microcontroller. Syringes up to 10 mL in volume are carried by a 3D-printed enclosure along a linear stage which is mounted to the RSA arm.

The fluid injector described here was designed to fit within a number of hardware components to enable multiple subtask automation of the dVRK Surgical Robot. The injector (and any other digital device within the surgical field) has an address on the i2c communication bus controlled by a master point which acts as a Robot Operating System (ROS) node.

V. Tumor Resection Experiments

Tumor resection includes four sub tasks: *Palpation*, *Incision*, *Debridement*, and *Injection*. Palpation of tissues is a

Preprint submitted to 2016 IEEE International Conference on Robotics and Automation. Received September 15, 2015.

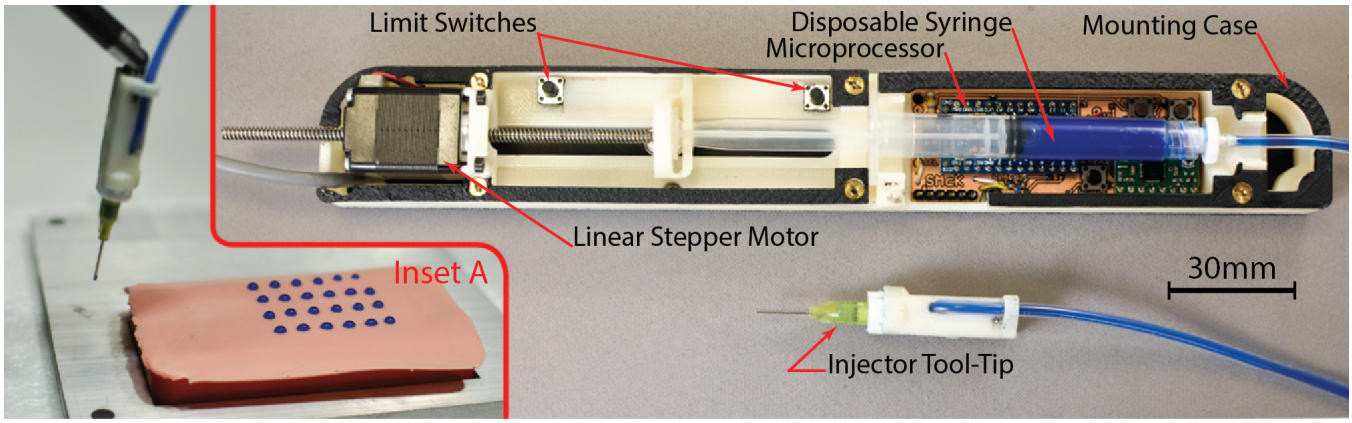

Fig. 5: The surgical injector is a stand-alone unit attached to a robotic surgical assistant. A dispensing tip is mounted to the surgical retractor using a mounting system shown in Figure 1(c).

means by which surgeons verify the location of tumors to make precise incisions using their sense of touch. Retraction and debridement require the interaction of the dVRK with flexible tissues. Surgical adhesive applications require the placement of discrete amounts of fluid to precise locations.

Experimental Setup: The palpation probe was affixed to the 8mm Needle Driver by manually placing the clevis-mounted probe below the surgical retractor, then prompting the jaws to open. The location of the flesh phantom was registered to the dVRK robot by manually tele-operating to the corners of the phantom and recording the global robot pose when palpation probe end effector distance was non-zero. These recorded points were used to fit a plane to the surface of the tissue. An aluminum indexing mount was fabricated and affixed within the workspace of the dVRK as shown in Figure 1.

Palpation: The dVRK retractor manipulates a palpation probe (as shown in Figure 3(d)) affixed to a modular instrument-tip mount to search for inclusions within a tissue phantom. The dVRK slides the lubricated end effector of the probe over the surface of the tissue in eight parallel passes while the end-effector deflection is recorded by the ROS. Each parallel pass covers the entire 150 mm length of the tissue phantom (details in [26]). In each palpation pass the relatively stiff tumor causes a local maxima in end-effector displacement indicating the position of the tumor. Robot position data associated with the probe deflection data is used to filter out noisy data near the edges of the tissue where the probe loses contact with the surface of the tissue. In Figure 6(a), a haptic probe is shown palpating a flesh phantom; the position estimate of the underlying tumor is shown in the inset.

Incision: The surgical retractor is prompted to close and the palpation probe is detached and replaced with a clevis-mounted type-15 scalpel shown in Figure 1(b). A linear incision is made in the cutaneous phantom at a fixed offset from the estimated location of the tumor to create a retractable flap. The incision is performed in 1 cm linear slicing motions rather than incising continuously in one single pass because of friction at the blade-silicone interface. Once all the segments are complete, a finishing pass is made along the full length of the incision to ensure a single continuous incision.

Without jaw articulation, this instrument is used to cut only in lines parallel to the 'y' axis. A third redesign allows for full articulation (similar to the mount shown in Figure 3(e)).

Debridement - Retraction and Resection: The next step in the pipeline is *Debridement*: after removing the clevis-mounted scalpel, the left retractor grasps the cutaneous flap created during incision by moving to a pose below the surface of the tissue and closing the jaws then *retracting* the skin to reveal the tumor. The right arm approaches the tumor and uses repeated grasping-and-retracting motions to incrementally *resect* the tumor from the subcutaneous tissue before removing it from the workspace. Depth of each arm is controlled as offsets from the surface plane created during indexing.

Injection: In the final step, the clevis-mounted injector tip (shown in Figure 1(c) connected to the Fluid Injection Device shown in Figure 5) is affixed to the surgical retractor on the right. The left surgical retractor then restores the skin flap to its original location before opening its jaws and depressing the cutaneous layer to stabilize the wound. The right arm uses the Fluid Injector to seal the incision with surgical adhesive. The needle tip passes over the incision at a constant rate as the externally mounted syringe pump injects the adhesive to facilitate uniform coverage of the incision site.

VI. Design of Tissue Phantoms

Tissue phantoms as shown in Figure 6 were created for testing. A cylindrical tumor of Silicone Rubber (thickness 3 mm; Shore hardness 70A) was coated in Vaseline and placed in the bottom of a 100 mm long, 50 mm wide, 20 mm deep *Delrin* mold prior to casting. Silicone Rubber *Ecoflex 00-30* (*Smooth-On*) was cast into the mold to create subcutaneous tissue. After setting, the subcutaneous phantom was demolded and inverted. A cutaneous phantom was created using a stiffer (shore hardness 2A) *DragonSkin 10 Medium* Silicone Rubber (*Smooth-On*). Opaque pigmentation was achieved using a 0.5% by volume addition of Oil Pigment (Winton Oil Colour, Flesh Tint). The dermal layer was cast at a thickness of 1 mm into a *Delrin* mold (width 60 mm

Preprint submitted to 2016 IEEE International Conference on Robotics and Automation. Received September 15, 2015.

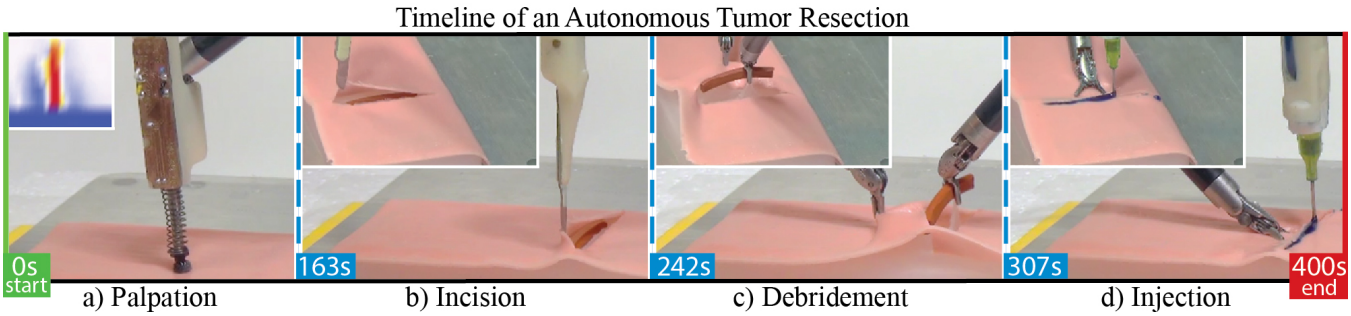

Fig. 6: An autonomous simulated-tumor resection was performed using our suite of interchangeable instrument-tips and the da Vinci 8 *mm* Needle Driver; the dVRK performed a) Palpation with a haptic probe, b) Incision using a scalpel, c) Debridement using the Needle Drivers, and d) Injection of a surgical adhesive. Full video of the task is available at: http://berkeleyautomation.github.io/surgical-tools

TABLE II: Autonomous Tumor Resection Open-Loop Automation Results and Sub-Task Timing (min:sec). The cause of failure for each trial is shaded in dark red. Visual feedback for the *Skin Retraction* subtask was implemented and raised success rates for the skin retraction phase to 100%. Visual feedback for tumor resection was implemented but did not yield more accuracy than palpation alone.

	start	Palpation	Tool Change	Incision	Tool Change	Debridement: Skin Retraction	Debridement: Tumor Resection	Tool Change	Injection	end
Trial 1		1:58	0:17	0:43	0:04		failed (0:31) - incorrect palpation estimate			FAILURE
2		1:58	0:18	0:51	0:03		0:49	0:11	1:03	SUCCESS
3		1:58	0:12	0:48	0:03		0:47	0:08	1:02	SUCCESS
4		1:58	0:15	0:47	0:06	failed (0:24) - improper skin retraction				FAILURE
5		1:58	0:19	0:55	0:03		0:49	0:06	1:06	SUCCESS
6		1:58	0:13	failed - incorrect palpation estimate						FAILURE
7		1:58	0:23	0:52	0:06	failed (0:29) - skin not grasped				FAILURE
8		1:58	0:23	0:51	0:03		failed (0:45) - tumor not grasped			FAILURE
9		1:58	0:17	0:56	0:03		0:51	0:08	1:05	SUCCESS
10		1:57	0:11	0:51	0:04		0:49	0:12	1:05	SUCCESS

and length 100 mm). Upon solidification, the dermal phantom was overlaid on the subcutaneous phantom to create the final tissue phantom setup.

VII. dVRK: Hardware and Software

We use the Intuitive Surgical da Vinci Research Kit (dVRK) as described in [30] along with open-source electronics and software developed by WPI and Johns Hopkins University [19]. The software system is integrated with ROS, and controls robot pose in Cartesian space by interpolating between requested points. Our manually created finite state machine consists of four segments with a tool change occurring between each as described in Figure 6.

VIII. Experimental Results

Tumor Resection End-to-End Performance: The end-to-end tumor resection was repeated ten times with no prior knowledge of tumor location. Each phantom had a skin-phantom layer of thickness (1 mm +/- 0.25 mm), tumor-phantom 25 mm in length and 3 mm in diameter. Success was determined based on a complete tumor removal and wound closure as shown in Table II. During trial 1 and trial 6, the position of the tumor was incorrectly estimated by the palpation probe resulting in respective failures in *Debridement* and *Incision*. In trial 4 and 7, the left retractor failed to grasp the dermal phantom fully and the tumor was not uncovered during skin retraction. In trial 8, the tumor was not fully resected from the flesh phantom during *Debridement*. Five of the ten trials were successful.

Visual Feedback: As seen in Table II four of the five failures occurred in the debridement sub-task with two of these due to failure of the jaws to properly retract the skin layer before extracting the tumor. The system is sensitive to the insertion depth, which also varies with skin thickness, which varies from $1-2$ mm. Insertion too deep can cause pinching of the layer beneath the skin, preventing retraction, and if too shallow the jaws will fail to grasp the skin layer. We used the open-cv computer vision toolkit to create a visual feedback filter to detect if the tumor is properly revealed by thresholding on color in the zone below the gripper. If the tumor is not visible, the system increases the insertion depth by 1 mm and makes another attempt. In ten independent trials the system succeeded the first time only once. Eight trials required two attempts, and one trial required three attempts. All trials were able to successfully complete debridement with visual feedback. In future work we will incorporate more visual feedback conditions.

Palpation Subtask Evaluation: Metrics such as sensitivity to speed, sliding direction, inclusion diameter, and inclusion depth were evaluated in a prior study by the authors using a probe similar to that shown in Figure 1(a) [26].

Incision Subtask Evaluation: The scalpel attachment for the clevis-mount was successfully used in nine of the ten recorded trials shown in Table II while cutting through 1 mm thick silicone phantom skin. Incision failed (in the sixth trial) when palpation data created an incorrect target estimate.

Debridement Subtask Evaluation: A flesh phantom with

tumors of known position and varying diameter (1, 2, 3 and 4) mm was created to test the efficacy of debridement strategies. We found in all trials that a single retraction (grasp-and-pull) attempt was insufficient to resect the tumor from the flesh phantom. Using two attempts increased efficacy to 75%, and three attempts were successful in all of 20 trials.

Sensitivity to tumor diameter was tested using a 3-grasp-and-retract strategy on tumors of (1, 2, 3, and 4) mm. Retraction was successful in all of ten trials on each of the 1 mm, 2 mm, and 3 mm tumors; none of the 10 attempts for the 4 mm tumor were successful.

Sensitivity to approach accuracy to proper palpation-localization estimate was tested by offsetting the horizontal approach of the retractor by (0, 1, and 2) mm. After establishing a baseline approach that was successful in 10 out of 10 debridement trials at 0 mm horizontal offset, the success rate dropped to 25% at 1 mm offset, and 0% at 2 mm approach offset. This result suggests that the palpation estimate is within 1 mm from the true position. Debridement results may benefit from visual feedback.

Fluid Injection Subtask Evaluation: To test precision of volume injection, an array of small droplets was injected with the Fluid Injector (shown in Figure 1(c)) onto an even surface and were visually measured by area from above; 24 drops were deposited at a mean overhead surface area of 37 mm^2 with 1.7 mm^2 standard deviation. A grid array target pattern was created to test the positional accuracy of the injection instrument and to evaluate its use in a tele-operated setting. The dVRK injected a pattern of droplets in a 3-by-3 grid covering an area of 20x16 mm which was visually graded and compared to an expert demonstration provided by a surgeon who had been asked to place the same pattern of droplets via tele-operation of the dVRK in a 10x10 mm area by sight. The expert demonstration had an average deviation from desired droplet position of 1.6 mm over 8 droplets; the autonomous injection was had an average deviation of 1.4mm over 8 droplets. These results suggest that the injection tool was useful in both tele-robotic and supervised autonomous control.

IX. Discussion and Future Work

We evaluated our design on the dVRK with da Vinci Classic Large Needle Driver instruments.

To explore automation of the multi-step tumor resection procedure, we describe the design of two novel devices and experiments. The first device is an interchangeable instrument mount which can use the jaws and wrist of a standard RMIS gripping tool to securely hold and manipulate a variety of end-effectors. The second is a fluid injection system which facilitates precision delivery of fluidic material such as chemotherapy, stem cells, and surgical adhesives to specific targets via a single-use needle attached to the interchangeable instrument mount. Fluid flow through the needle is controlled via an externally-mounted automated lead screw. Experiments suggest that an automated version of the Intuitive Surgical dVRK system using these devices, combined with a palpation probe and sensing model described in a previous paper, can successfully complete the entire procedure in approximately half the trials, and that the most common failure phase, debridement, can be improved with visual feedback. Design files and fabrication instructions are available online at: http://berkeleyautomation.github.io/surgical-tools/.

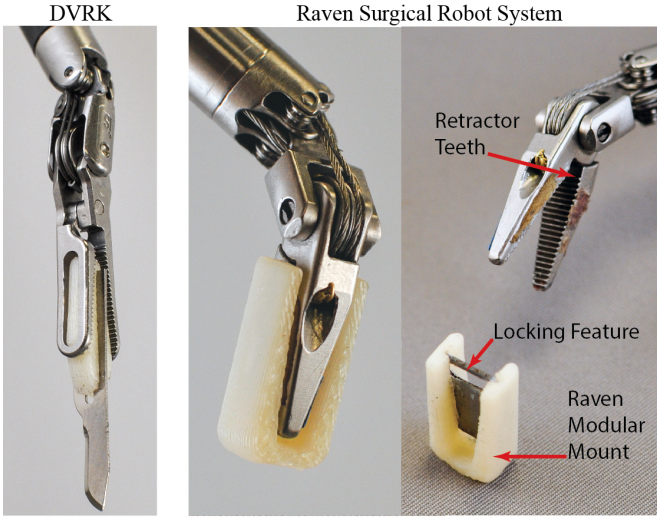

a) Fenestrated Jaw Mount

b) Modular Raven Retractor Mount

Fig. 7: Mount designs for the Fenestrated Jaw Retractor and Raven Surgical Retractor Instruments.

In future work: We will incorporate visual feedback and perform experiments to evaluate force and torque resistance of the mounts (which are challenging due to the fragility and limited availability of classic da Vinci Large Needle Drivers). We will also extend these designs to other end-effectors, such as the da Vinci Fenestrated Retractor shown in a very preliminary version in Figure 7(a). The small oval "windows" in each jaw may allow protrusions on the mount to act as indexing features. We will also design and evaluate interchangeable mounts for the Raven II Robotic Surgical Assistant system using the proximal retractor teeth of the Raven II jaws as indexing features to mate with a custom designed locking feature (a 0.025 in steel plate) as shown in a very preliminary version in Fig 7(b).

Acknowledgements

This research was performed in the CAL-MR (Center for Automation and Learning for Medical Robotics) and in UC Berkeley's Automation Sciences Lab under the UC Berkeley Center for Information Technology in the Interest of Society (CITRIS) "People and Robots" Initiative: (robotics.citris-uc.org). This work was supported in part by the U.S. National Science Foundation under NRI Award IIS-1227536: Multilateral Manipulation by Human-Robot Collaborative Systems; and by Google, Cisco, a major equipment grant from Intuitive Surgical and by generous donations from Andy Chou and Susan and Deepak Lim. We also thank Pieter Abbeel, Allison Okumura, W. Doug Boyd MD, Simon DiMaio, Jeff Mahler, Michael Laskey, Zoe McCarthy, Meng Guo, and Florian T. Pokorny who provided helpful feedback.

REFERENCES

[1] "Intuitive Surgical, da Vinci Research Kit." [Online]. Available: http://research.intusurg.com/dvRK

[2] "Intuitive Surgical, EndoWrist®/Single-Site® Instrument & Accessory Catalog." [Online]. Available: http://www.intuitivesurgical.com/products/871145_Instrument_Accessory_%20Catalog.pdf

[3] R. Alterovitz and K. Goldberg, *Motion Planning in Medicine: Optimization and Simulation Algorithms for Image-guided Procedures*. Springer, 2008.

[4] J. Alvarez, G. Stahler, F. Barbagli, and C. Carlson, "Endoscopic robotic catheter system," Jan. 20 2011, US Patent App. 12/504,559.

[5] *ST79-Comprehensive guide to steam sterilization and sterility assurance in health care facilities,*, ANSI/AAMI Std. ST79:2010/A4:2013.

[6] C. E. Attinger, E. Bulan, and P. A. Blume, "Surgical Debridement: The Key to Successful Wound Healing and Reconstruction," *Clinics in podiatric medicine and surgery*, vol. 17, no. 4, p. 599, 2000.

[7] R. A. Beasley, "Medical Robots: Current Systems and Research Directions," *Journal of Robotics*, vol. 2012, 2012.

[8] A. Darzi and Y. Munz, "The impact of minimally invasive surgical techniques," *Annu. Rev. Med.*, 2004.

[9] G. Dulan, R. V. Rege, D. C. Hogg, K. M. Gilberg-Fisher, N. A. Arain, S. T. Tesfay, and D. J. Scott, "Developing a Comprehensive, Proficiency-based Training Program for Robotic Surgery," *Surgery*.

[10] Y. Fong, W. Jarnagin, K. Conlon, R. DeMatteo, E. Dougherty, and L. Blumgart, "Hand-assisted laparoscopic liver resection: Lessons from an initial experience," *Archives of Surgery*, 2000.

[11] D. C. Friedman, J. Dosher, T. Kowalewski, J. Rosen, and B. Hannaford, "Automated tool handling for the trauma pod surgical robot," in *ICRA*, 2007.

[12] M. Granick, J. Boykin, R. Gamelli, G. Schultz, and M. Tenenhaus, "Toward a Common Language: Surgical Wound Bed Preparation and Debridement," *Wound repair and regeneration*, 2006.

[13] R. Hambley, P. A. Hebda, E. Abell, B. A. Cohen, and B. V. Jegasothy, "Wound healing of skin incisions produced by ultrasonically vibrating knife, scalpel, electrosurgery, and carbon dioxide laser," *The Journal of Dermatologic Surgery and Oncology*, vol. 14, no. 11, 1988.

[14] B. Hannaford, J. Rosen, D. W. Friedman, H. King, P. Roan, L. Cheng, D. Glozman, J. Ma, S. N. Kosari, and L. White, "Raven-ii: an open platform for surgical robotics research," *Biomedical Engineering, IEEE Transactions on*, 2013.

[15] D. Hu, Y. Gong, B. Hannaford, and E. J. Seibel, "Semi-autonomous simulated brain tumor ablation with ravenii surgical robot using behavior tree," in *IEEE Int. Conf. Robotics and Automation*, 2015.

[16] Intuitive Surgical, "Annual report 2014." [Online]. Available: http://investor.intuitivesurgical.com/phoenix.zhtml?c=122359&p=irol-IRHome

[17] Y. Jung, G. Bauer, and J. A. Nolta, "Concise review: Induced pluripotent stem cell-derived mesenchymal stem cells: progress toward safe clinical products," *Stem cells*, vol. 30, no. 1, pp. 42–47, 2012.

[18] J. M. Karp and G. S. L. Teo, "Mesenchymal stem cell homing: the devil is in the details," *Cell stem cell*, vol. 4, no. 3, pp. 206–216, 2009.

[19] P. Kazanzides, Z. Chen, A. Deguet, G. S. Fischer, R. H. Taylor, and S. P. DiMaio, "An open-source research kit for the da vinci® surgical system," in *IEEE Int. Conf. Robotics and Automation (ICRA)*, 2014.

[20] B. Kehoe, G. Kahn, J. Mahler, J.-H. Kim, A. Lee, K. Nakagawa, S. Patil, W. D. Boyd, P. Abbeel, and K. Goldberg, "Autonomous multilateral debridement with the raven surgical robot," in *ICRA*, 2014.

[21] T. Kheir, "Multi-purpose minimally invasive instrument that uses a micro entry port," Feb. 23 2010, uS Patent 7,666,181.

[22] J. Konstantinova, A. Jiang, K. Althoefer, P. Dasgupta, and T. Nanayakkara, "Implementation of tactile sensing for palpation in robot-assisted minimally invasive surgery: A review," *Sensors Journal, IEEE*, 2014.

[23] M. Kranzfelder, C. Staub, A. Fiolka, A. Schneider, S. Gillen, D. Wilhelm, H. Friess, A. Knoll, and H. Feussner, "Toward increased autonomy in the surgical or: needs, requests, and expectations," *Surgical endoscopy*, 2013.

[24] C. Kucur, K. Durmus, P. T. Dziegielewski, and E. Ozer, "Transoral robot-assisted carbon dioxide laser surgery for hypopharyngeal cancer," *Head & neck*, 2015.

[25] P. Losi, S. Burchielli, D. Spiller, V. Finotti, S. Kull, E. Briganti, and G. Soldani, "Cyanoacrylate surgical glue as an alternative to suture threads for mesh fixation in hernia repair," *Journal of Surgical Research*, 2010.

[26] S. McKinley, A. Garg, S. Sen, R. Kapadia, A. Murali, K. Nichols, S. Lim, S. Patil, P. Abbeel, A. M. Okamura, and K. Goldeber, "A disposable haptic palpation probe for locating subcutaneous blood vessels in robot-assisted minimally invasive surgery," in *CASE*, 2015.

[27] S. McKinley, S. Sen, A. Garg, Y. Jen, D. Gealy, P. Abbeel, and K. Goldberg, "Autonomous Tumor Localization and Extraction: Palpation, Incision, Debridement and Adhesive Closure with the da Vinci Research Kit," Hamlyn Surgical Robotics Conference, London.

[28] D. J. Miller, C. A. Nelson, and D. Oleynikov, "Shortened OR time and decreased patient risk through use of a modular surgical instrument with artificial intelligence," *Surgical endoscopy*, vol. 23, 2009.

[29] G. Moustris, S. Hiridis, K. Deliparaschos, and K. Konstantinidis, "Evolution of autonomous and semi-autonomous robotic surgical systems: a review of the literature," *The International Journal of Medical Robotics and Computer Assisted Surgery*, 2011.

[30] A. Murali, S. Sen, B. Kehoe, A. Garg, S. McFarland, S. Patil, W. D. Boyd, S. Lim, P. Abbeel, and K. Goldberg, "Learning by observation for surgical subtasks: Multilateral cutting of 3D viscoelastic and 2D orthotropic tissue phantoms," in *ICRA*, 2015.

[31] K. Nichols, A. M. Okamura, *et al.*, "Methods to segment hard inclusions in soft tissue during autonomous robotic palpation," *Robotics, IEEE Transactions on*, 2015.

[32] C. C. L. or Open Resection Study Group *et al.*, "Laparoscopic surgery versus open surgery for colon cancer: short-term outcomes of a randomised trial," *The lancet oncology*, 2005.

[33] N. Padoy and G. Hager, "Human-Machine Collaborative Surgery using Learned Models," in *ICRA*, 2011, pp. 5285–5292.

[34] S. Parihar, "Percutaneous instrument and method," Sept. 18 2014, US Patent App. 13/832,496.

[35] C. Penna, "Laparoscopic instruments, attachable end effectors and methods relating to same," Aug. 7 2014, US Patent App. 13/756,777.

[36] E. Ritter and D. Scott, "Design of a Proficiency-based Skills Training Curriculum for the Fundamentals of Laparoscopic Surgery," *Surgical Innovation*, vol. 14, no. 2, pp. 107–112, 2007.

[37] R. Smith, V. Patel, and R. Satava, "Fundamentals of robotic surgery: a course of basic robotic surgery skills based upon a 14-society consensus template of outcomes measures and curriculum development," *The International Journal of Medical Robotics and Computer Assisted Surgery*, vol. 10, no. 3, pp. 379–384, 2014.

[38] J. Spivey, K. Huey, R. Nobis, and S. Conlon, "Method for exchanging end effectors in vivo," Apr. 14 2011, US Patent App. 12/576,578.

[39] D. Stoianovici, J. A. Cadeddu, R. D. Demaree, S. A. Basile, R. H. Taylor, L. L. Whitcomb, *et al.*, "An efficient needle injection technique and radiological guidance method for percutaneous procedures," in *CVRMed-MRCAS'97*. Springer, 1997.

[40] E. Tateishi-Yuyama, H. Matsubara, T. Murohara, U. Ikeda, S. Shintani, H. Masaki, K. Amano, Y. Kishimoto, K. Yoshimoto, H. Akashi, *et al.*, "Therapeutic angiogenesis for patients with limb ischaemia by autologous transplantation of bone-marrow cells: a pilot study and a randomised controlled trial," *The Lancet*, vol. 360, 2002.

[41] R. Taylor, A. Menciassi, G. Fichtinger, and P. Dario, "Medical Robotics and Computer-Integrated Surgery," *Springer Handbook of Robotics*, pp. 1199–1222, 2008.

[42] Teleflex, "Teleflex press release." [Online]. Available: http://phx.corporate-ir.net/phoenix.zhtml?c=84306&p=irol-newsArticle_print&ID=2025774

[43] S. Thielmann, U. Seibold, R. Haslinger, G. Passig, T. Bahls, S. Jörg, M. Nickl, A. Nothhelfer, U. Hagn, and G. Hirzinger, "Mica-a new generation of versatile instruments in robotic surgery," in *Intelligent Robots and Systems (IROS), 2010 IEEE/RSJ International Conference on*. IEEE, 2010, pp. 871–878.

[44] M. Velez, J. Velez, and A. Velez, "Surgical staple and endoscopic stapler," Feb. 28 1995, US Patent 5,392,978.

[45] A. Wolf and M. Shoham, "Medical Automation and Robotics," in *Springer Handbook of Automation*, 2009, pp. 1397–1407.